Plasma degradation of water organic pollutants: Ab-initio molecular dynamics simulations and experiments

Pascal Brault, Florin Bilea, Monica Magureanu, Corina Bradu, Olivier Aubry, Hervé Rabat, Dunpin Hong, Florin Bilea, Monica Magureanu, Corina Bradu, et al.

Received: Added at production | Revised: Added at production | Accepted: Added at production

DOI: xxx/xxxx

RESEARCH ARTICLE

Plasma degradation of water organic pollutants: Ab-initio molecular dynamics simulations and experiments

Pascal Brault*[1] | Florin Bilea[2] | Monica Magureanu[2] | Corina Bradu[3] | Olivier Aubry[1] | Hervé Rabat[1] | Dunpin Hong[1]

[1]GREMI, CNRS - Université d'Orléans, 14 rue d'Issoudun, Orléans, 45067, France
[2]Department of Plasma Physics and, Nuclear Fusion, National Institute for Lasers, Plasma and Radiation Physics, Atomistilor Str. 409, P.O. Box MG-36, Bucharest, 077125,Romania
[3]Department of Systems Ecology and Sustainability, Faculty of Biology, University of Bucharest, Splaiul Independentei 91-95, Bucharest, 050095, Romania

Correspondence
*Pascal Brault Email: pascal.brault@univ-orleans.fr

Summary

Ab-initio molecular dynamics simulations and experiments was carried out for studying the interaction between plasma-produced hydroxyl radical and organic pollutant molecules in wastewater. The simulation method was validated on the degradation products of phenol and further applied to the more complex molecule of sulfamethoxazole (SMX). The comparison with experimentally detected intermediate products obtained during plasma treatment of SMX solutions confirms the hydroxylation of the benzene and isoxazole rings observed in some of the simulations

KEYWORDS:
reactive molecular dynamics, ab-initio molecular dynamics, cold atmospheric plasma, plasma oxidation, waste water treatment, phenol, sulfamethoxazole, SMX, antibiotics, tandem mass spectrometry

1 | INTRODUCTION

Eliminating pollutants in water is a world challenge that non-thermal plasmas at atmospheric pressure are aiming to address. Various plasma sources efficiently produce reactive oxygen and nitrogen species (RONS) that interact with and subsequently degrade organic molecules. Since such phenomena are molecular in nature, reactive classical and ab-initio molecular dynamics are relevant tools for analyzing involved degradative oxidation processes [1]. The main actor among the plasma-generated reactive oxygen and nitrogen species is the HO• radical, which efficiently and unselectively reacts with any organic molecule. The production of HO• in plasmas in contact with water is generally attributed to electron impact dissociation of water molecules. However, other formation mechanisms are also possible and some of them, such as dissociative recombination reactions, can have a major contribution to HO• generation depending on the specific plasma properties [2]. Regardless of the plasma source used for water treatment, HO• is acknowledged to play the main role in the degradation [3–5]. Actually, all advanced oxidation

processes (AOPs) rely on the formation of HO$^\bullet$ [6,7]. The simulations performed in this article are carried out for describing and predicting degradation products after interactions, in water, of selected molecules with HO$^\bullet$ radical, which is of crucial importance, since the products can also be harmful.

Molecular dynamics simulations (MD) are of growing interest for studying physical chemical processes in plasmas [8,9]. This interest is motivated by the ability of these simulations to address reactivity of relatively large molecular systems (up to 109 atoms). Since plasmas are able to produce radicals that interact with other species both in gas phase as well as with solid and liquid surfaces, including in-diffusion, MD simulations are relevant for tracking such reactive processes. Unfortunately, it is not yet possible to directly include the electrons in MD. Despite this limitation, neutral-neutral, ion-neutral and ion-ion interactions can be including with proper initial conditions such as positions and velocities, required for solving the MD Newton equations of motion. Moreover, these initial conditions can be defined using plasma composition from experimental measurements, such as mass spectrometry or from fluid model [10–13]. Solving these equations, only requires the knowledge of the interaction potentials, and then the forces between each interacting species. There are two popular reactive force fields families, able to describe chemical reactions: reaxFF and COMB3 [14], which address bond breaking and formation via a distance dependent bond order. Moreover, these force fields implement a variable charge scheme which allows to address charge transfer. The main limitation is that these forcefields are parametrized for a small set of molecules and they are not always transferable to any similar molecules or to other molecules containing the same atoms. When there is a lack of forcefields due to the complexity of the involved molecules, coupling quantum calculated forcefield calculations in MD simulations is the solution [15]. It is called Ab-Initio or First Principle Molecular Dynamics (AIMD or FPMD). Basically, the forcefields are calculated every defined timestep using a quantum chemistry code (such as Density Functional Theory (DFT) for example, but not limited to it), after which a MD step is achieved. The main difficulty is to choose the most appropriate quantum chemistry method and basis sets. The main limitation is the computing time which becomes very long when high accuracy is expected. The present work will thus address the interaction of HO$^\bullet$ radical with some selected molecules present in water, using Ab-Initio Molecular Dynamics (AIMD). For implementing this method, we are using the Density-Functional Theory (DFT) in the Tight-Binding approach (DFTB) which is a computationally efficient DFT scheme for the ab initio step of calculating the forces between atoms. Moreover, we use the GFN1-xTB parametrization, which is optimized for geometries, frequencies and non-covalent interactions and covers all elements of the periodic table up to radon [16]. For taking into account conditions of non-thermal plasma experiments, as closely as possible, Molecular Dynamic (MD) simulations are carried out at 300K with periodic release of HO$^\bullet$ radical into water containing the selected pollutant molecule: Phenol (C_6H_5OH) and Sulfamethoxazole ($C_{10}H_{11}N_3O_3S$) oxidation processes by HO$^\bullet$ in water are respectively investigated. Phenol is studied as test molecule for building and validating the AIMD approach since there are significant data in literature. An additional motivation for the selection of phenol is the toxicity of numerous phenolic compounds [17,18]. Sulfamethoxazole (SMX) is a widely used antibacterial antibiotics both in human healthcare and animal

breeding. It is present in water especially close to intensive farming areas [19–21], but also in hospital wastewater [22,23] and in the effluent from pharmaceutical plants [24]. Wastewater treatment plants fail to effectively remove SMX as proved by its presence in the treated effluents [23], and thus it is frequently found in surface waters [23,25,26], groundwater and tap water [23,27] and could pose an ecotoxicological risk to aquatic organisms [22] and contribute to the spread of antibiotic resistance [26]. For these molecules the MD simulated degradation products are compared with available experimental ones detected by liquid chromatography-tandem mass spectrometry (LC-MS/MS). Summarily, an AIMD simulation protocol is tested on a widely studied molecule, here phenol, and applied on a more complex molecules, here SMX. Comparison with literature and here reported experiments are presented.

2 | MOLECULAR DYNAMICS

Initial Simulation box size are 10x10x10 $Å^3$ comprising 1 phenol or 1 SMX molecule with 15 H_2O molecules. This small number of water molecules is expected to be enough for representing the environment of the SMX molecules [1]. 10 $HO^•$ radicals are released one after each other at random position with 2.5 Å minimum distance with molecules already in the box. Integration time dt = 0.25 fs and the simulation lasts for 5. 10^4 timesteps i.e. 12.5 ps. $HO^•$ are released every 4000 timesteps after an initial delay of 4000 timesteps. The simulations are carried out in the NPT ensemble (i.e. total atom number N, total pressure P and Temperature T are kept constant). This allows keeping a constant water density when releasing $HO^•$ radicals. A Nose-Hoover thermostat is used for maintaining the temperature at 300K. The damping time is 100 fs. A Martyna-Tobias-Klein barostat with damping time of 500 fs is used for maintaining the pressure at 10^5 Pa. Simulations are repeated 10 times after changing initial positions and velocities of all molecules at starting time minimal for statistical purposes. AIMD simulations have been carried using AMS suite from SCM company [28]

3 | EXPERIMENTS

The experiments on SMX degradation were performed using a pulsed corona discharge above water with gas recycling. The system is described in detail in previous articles [29,30] and consists of two reactors connected in series, i.e. the plasma reactor and the solution tank through where the effluent gas from the discharge is bubbled. This method ensures enhanced contact between the oxidizing species produced in the plasma and the pollutant molecules, and thus remarkably improves degradation efficiency [29]. Plasma-generated ozone plays a major role in this set-up. It can react directly with the organic contaminant, especially in the solution reservoir, where the bubbling considerably enhances the contact surface area as compared to the plasma reactor. More importantly, the peroxone process, i.e. the reaction between ozone and hydrogen peroxide produced in plasma generates additional $HO^•$ radicals outside of the plasma region. Previous results showed the formation of H_2O_2 in plasma-treated

water, but evidenced its absence in case of gas recycling, as well as the elimination of externally added H_2O_2 [31,32]. It was also observed that the concentration of HO radicals doubles in this set-up as compared to plasma alone [32]. The corona discharge was generated in oxygen (flow rate 300 mL/min), in multi-wire-to-plate configuration, using an array of 20 copper wires (diameter 100 μm) as high voltage electrode placed above the liquid surface, which is grounded. Based on a previous optimization study [33], high voltage pulses of 110 ns (full width at half maximum) and 18 kV amplitude were selected for these experiments. The pulse frequency was set to 25 Hz and under these conditions the power dissipated in the plasma was approximately 5 W. The sulfamethoxazole solution was prepared at a concentration of 0.5 mM in distilled water. The conductivity was adjusted to 300 μS/cm using $NaHCO_3$. A solution volume of 330 mL was treated for 60 min and samples were collected periodically (2, 5, 10, 20, 40 and 60 min) during the treatment. The pollutant concentration was measured by high performance liquid chromatography (HPLC) using a Rigol L-3000 system equipped with a RP-C18 column (250 x 4.6 mm, 5 μm) maintained at 27 °C. The mobile phase consisted of 30% acetonitrile and 70% water (with 0.1% formic acid). The measurements were done at 270 nm using a diode array detector. The degradation products of sulfamethoxazole were studied using an Agilent 1260 Infinity II HPLC coupled with a 6530 QTOF detector. The separation was achieved using an Eclipse C18 Plus column (150 x 3 mm, 3.5 μm) kept at 25°C. The mobile phase consisted of acetonitrile and water (with 0.1 % formic acid) and was varied over the course of 25 min from 5% to 20% acetonitrile, while maintaining a constant flow of 0.4 mL/min. The parameters of the electrospray ionization (ESI) source were set as follows: capillary voltage at 3500 V, nozzle voltage at 1000 V, gas temperature 300°C, gas flow 8 L/min, sheath gas temperature 350 °C, sheath gas flow 11 L/min, nebulizer 35 psig. MS and MS/MS spectra were recorded in the range 50-1000 (mass / charge), for both positive and negative ions, at a rate of 3 spectra / second and 1 spectrum / second respectively. The collision energy was varied between 0 and 20 eV.

4 | RESULTS

4.1 | Phenol

Phenol (C_6H_5OH) is one of the simplest cyclic molecules. Its oxidation degradation routes have been studied experimentally and there is a consensus on oxidation steps and products [34]. These experimentally determined steps and products are summarized in Fig. 1.

Phenol degradation has been studied in numerous plasma systems utilizing electrical discharges generated directly in water or in gas-liquid environments. A summary of this research with respect to the intermediate products and reaction mechanism is provided in [35]. The majority of the studies report that the plasma oxidation of phenol in water occurs through reaction with hydroxyl radicals which electrophillically attack the phenol molecule. The authors suggest the formation of a transient dihydroxycyclohexadienyl radical as a result of this attack, which may further react, finally leading to hydroxylated products of

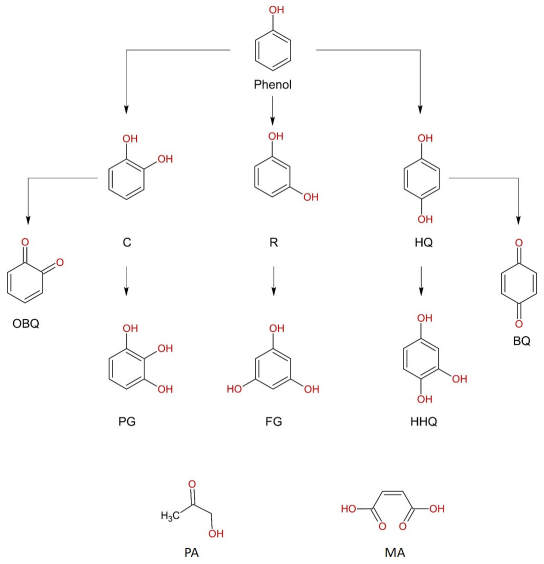

Figure 1 Summary of the reported phenol oxidation steps and corresponding products : catechol (C), resorcinol (R), hydroquinone (HQ), 1,4-benzoquinone (BQ), 1,2-benzoquinone (OBQ), pyrogallol (PG), phloroglucinol (FG), hydroxyhydroquinone (HHQ), pyruvic acid (PA), maleic acid (MA). Adapted from Ref. [34]

phenol such as catechol, hydroquinone and benzoquinone. Further oxidation of these intermediates to trihydroxybenzenes such as pyrogallol, hydroxyhydroquinone and phloroglucinol represents the next step in the reaction pathway. Various ring cleavage products were also typically reported in phenol solutions exposed to plasma, the most frequent being organic acids such as maleic, oxalic and formic acids.

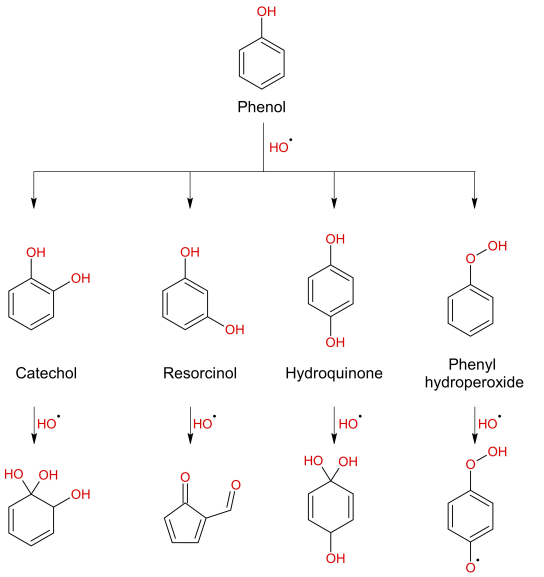

Figure 2 MD simulations obtained products after interaction with HO•

AIMD simulations consist of 10 runs with different random initial conditions for positions and velocities. The latter are randomly selected in a Maxwell-Boltzmann distribution at temperature 300K. The first oxidation step by HO• leads to 4 catechol (C), 4 resorcinol (R), 1 Hydroquinone (HQ) and 1 Phenyl hydroperoxide) molecules, when analyzing the 10 run results (Fig. 2). When looking at the next steps, 3 hydroxyhydroquinone (HHQ) and 2 pyrogallol (PG) are created in 5 of the 10 runs (not shown in Figure 2). In the 5 other remaining runs 4 molecules are created as shown in Figure 2. These molecules are evolving towards cycle breaking after additional HO• release, while HHQ and PG are rather further hydroxylated. When comparing Figures 1 and 2, this phenol oxidation study, using AIMD, is thus able to reproduce main phenol oxidation products. So the present simulation protocol can be applied to a more complex organic pollutants, here sulfamethoxazole.

4.2 | Sulfamethoxazole

4.2.1 | Experiments

Figure 3 shows the degradation of SMX in water, more precisely the variation of the relative concentration and the logarithmic representation (inset) as a function of plasma treatment time. The decrease in concentration is well described by a first order decay exponential function. The first order kinetics is confirmed by the logarithmic representation, with an apparent reaction rate constant $k_{obs} = 0.205\ \text{min}^{-1}$. Almost complete removal of the initial 0.5 mM SMX was achieved after 20 min exposure to plasma, while the half life time (i.e. the time needed to degrade half of the initial concentration of contaminant) was approximately 5 min. A useful parameter for evaluating the treatment efficiency is the energy yield, defined as the amount of contaminant removed per unit of energy spent in the process and usually measured either at 50% or, more frequently, at 90% removal of the target compound. In our case, a value of 32 g/kWh was obtained at 90% SMX removal.

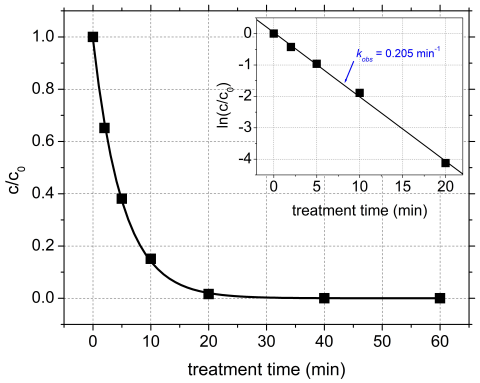

Figure 3 Decrease of SMX concentration as a function of time. Inset: logarithmic representation of the degradation as a function of treatment time.

Identification of sulfamethoxazole degradation products was done based on the MS/MS fragmentation patterns recorded. Several hydroxylated compounds have been observed and they are represented in Figure 4. The only compounds detected in the solution as a result of treatment are the ones on the first row, referred as P1 to P5. The masses of the products, as seen in the solution, are P1-269 amu, P2- 285 amu, P3-301 amu, P4-269 amu, P5-287 amu, all of them detected either as positive ions (+1 amu) or negative ions (-1 amu). The second and third rows in Figure 4 are fragments of these compounds obtained during the analysis as a result of the fragmentation in the electrospray ionization source. When considering the HO• reaction with sulfamethoxazole, the two cycles in the compound's structure (the benzene and isoxazole rings) appear to act independently of each other. As such, the degradation products can be grouped based on the attack site of HO• in two degradation paths: hydroxylation of benzene (P1-P3) and hydroxylation of the isoxazole ring (P4-P5). The first path starts with the formation of compound P1 (2 isomers) with a mass spectrum containing the m/z+ values 172, 124, 108. These fragments are consistent with the presence of a hydroxyl group on the benzene ring as shown in Figure 4. Using the same reasoning, the di-hydroxylated P2 and tri-hydroxylated P3 have been identified. The mass spectrum of P2 contains fragments with m/z- values of 137 and 122, while the one attributed to P3 includes m/z- 204 and 140 and m/z+ 140 and 123. Thus, the HO• attack on the benzene ring describes a sequential hydroxylation of sulfamethoxazole. The attach of HO• on the isoxazole ring initiates the second degradation path. In this case, the formation of the mono-hydroxylated P4 degradation product was confirmed due to the presence of the 115 m/z+ fragment in the compound's mass spectrum. The addition of a HO• to P4 results in the formation of P5. During its fragmentation, the compound loses a water molecule and forms the m/z+ 270 ion, which undergoes C-N bond cleavage resulting in m/z+ 96 ion.

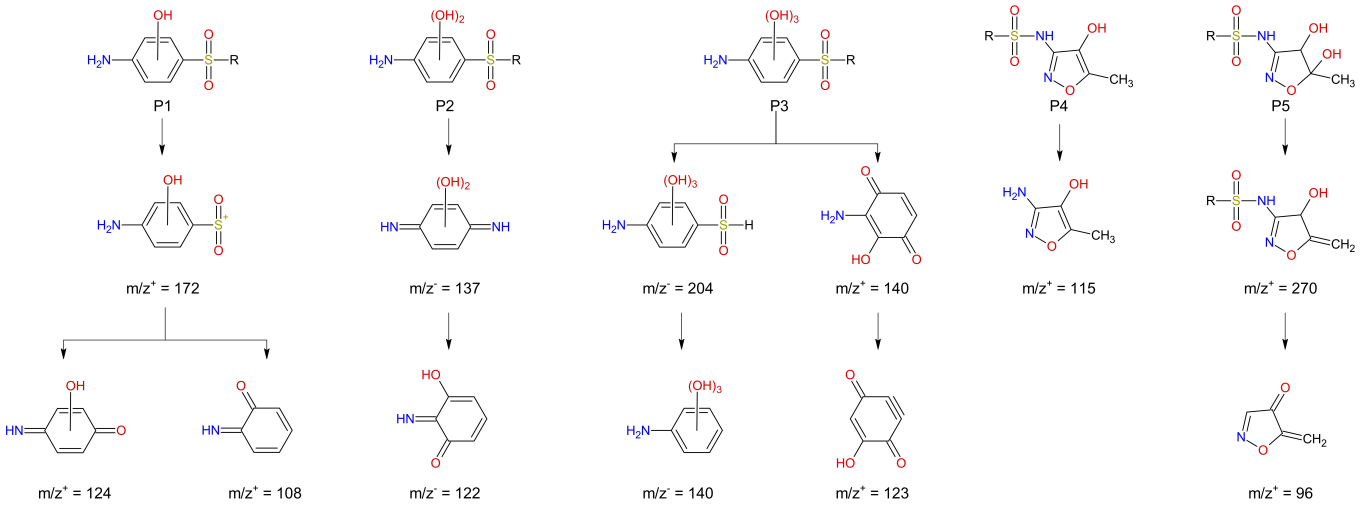

Figure 4 MS/MS fragmentation patterns of the hydroxylated degradation products of sulfamethoxazole obtained during plasma treatment.

Table 1 List of the masses (amu) after HO$^\bullet$ release. m_i is/are the mass(es) obtained after injection of the i^{th} HO$^\bullet$ in the corresponding time interval (in the form $t_i - t_{i+1}$ps). Bold masses are confirmed by experiments. Underlined masses have a potential match

	m_0 0-1ps	m_1 1-2ps	m_2 2- 3ps	m_3 3-4ps	m_4 4-5ps	m_5 5-6ps	m_6 6-7ps	m_7 7-8ps	m_8 8-9ps	m_9 9-10ps	m_{10} 10-12.5ps
Run #1	253	252	269	268	267	267	266	265	282	299	315
Run #2	253	**269**	**269**	268	**285**	284	301	299	299	298	315
Run #3	253	252	269	286	285	302	301	318	301	300	285
											32
Run #4	253	253	**269**	268	268	251	251	251	285	333	333
Run #5	253	252	**269**	**269**	108	108	126	126	125	123	140
					176	176	192	192	192	192	192
Run #6	253	253	**269**	268	285	302	319	336	157	156	70
									195	195	103
											196
Run #7	253	253	**270**	286	302	302	303	320	319	318	317
Run #8	253	**270**	269	268	267	284	63	63	317	81	82
							237	236		253	269
Run #9	253	252	**269**	286	303	320	337	336	157	174	173
									196	196	196
Run #10	253	253	269	269	269	269	269	269	269	285	317

4.2.2 | Ab-initio Molecular Dynamics

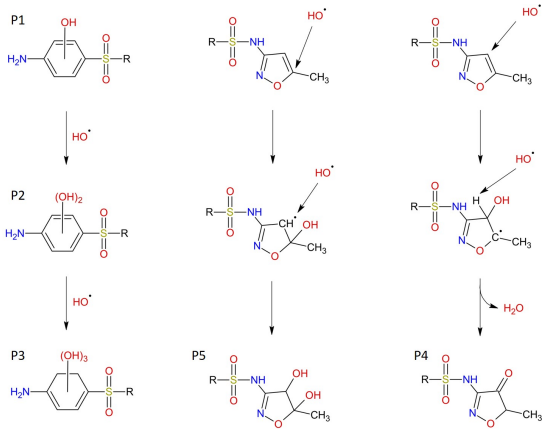

Figure 5 The main hydroxylation reactions observed during the simulations of sulfamethoxazole oxidation leading to observed products P1-P5 of Fig. 4

SMX oxidation process in water is calculated using the previous AIMD procedure for phenol, i.e. 10 runs with different initial conditions, as for phenol in the previous section. The HO$^\bullet$ radical is injected every 1 ps and 10 times. 1 ps relaxation is ran before the first HO$^\bullet$ injection and 2.5 ps is lasting after the tenth released HO$^\bullet$. Table 1 displays recorded masses of compounds issued

from SMX, that can be further compared to mass spectrometry measurements. Bold numbers correspond to masses recorded in the present experiments and underlined ones have a potential match. Fig. 5 shows chemical structures corresponding to main AIMD simulated hydroxylated products. Resulting simulated product mass ranges 265-270, 282-286, 298-303 (all runs) are corresponding to hydroxylation with 1, 2 and 3 HO• respectively, either on benzene ring or isoxazole ring, as in experiments. AIMD simulations predict mass in the range of 315-319 and 335-336 corresponding to 4 and 5 additional attached HO• to SMX. Such mass ranges, 3 to 5 atomic mass units wide are issued from transient situations with unrelaxed compounds. For comparison, with mass spectrometry measurements, results can differ from some unit values, without being false. From Table 1, larger masses are resulting in fragmentation of these multiple hydroxylated SMX. S-C bond breaking occurs after HO• impacting on S, SO or C atom adjacent to S atom to give dissociation to fragments of mass 108 to 196. Fragmentation occurs (masses less than 253 amu) during 4 runs over the 10 submitted. In one occurrence, three fragments are obtained (run #7).

5 | DISCUSSION

Main recorded high masses (> 253 amu) have been already reported in experiments such as ultrasound/ozone oxidation process[19], photocatalytic[36], non-thermal-plasmas[4,37–45] and combination of advanced oxidation processes[46]. Most of the AIMD simulations and present experimental results show changes of either or both cycles, while the S-N bond is rarely affected. As such, the two cycles can be treated as separate entities which can react with hydroxyl radicals alternatively or simultaneously, leading to the formation of several mono-, di-, tri-, tetra- and penta- hydroxylated compounds over the course of the AIMD simulations. Hydroxylation of the benzene ring (Figure 5) occurs as one of the first steps during degradation. This leads to the formation of several isomers depending on the attack site of the hydroxyl radicals. As a result of plasma driven sulfamethoxazole degradation, at least two of these isomers are formed, having a mass of 269 amu. Formation of these isomers was observed in simulation runs #4 and #9. The attack of hydroxyl radicals on the isoxazole ring occurs alternatively on either side of the C=C bond, forming the mono-hydroxylated P4 (run #6, #8) and the di-hydroxylated P5 (run #7, #9). Benzene hydroxylation occurs simultaneous with the hydroxyl attack on the isoxazole cycle during simulation runs #2, #3, #6, #7, #8 and #9. Comparison of Fig. 4 and Fig. 5 thus shows a reasonable agreement between AIMD and MS/MS experiments regarding hydroxylation steps. However, the fragmentation of the pollutant molecule observed in AIMD as the fragment masses 63, 70, 81-82, 108, 124, 140, 157, 172-174 could not be corelated with the experimental results. Nevertheless, fragment masses 108, 156, 172 have been previously detected (Fig. 12 and 13 from Ref.[20]). It is possible that fragments formed during plasma degradation of sulfamethoxazole are not detected with the chromatographic method employed. It should also be mentioned that, while AIMD accounts for the contribution of hydroxyl radicals towards pollutant removal, plasma also generates a series of other reactive species (ozone, hydrogen peroxide, hydroperoxyl radical, etc.) which could be involved in the degradation of sulfamethoxazole

generating different degradation products than HO• [47].Thus, a perfect correlation can not be expected. Another explanation for the observed discrepancies could stem from the timeline of the reactions. During the plasma experiments, the abundance of the pollutant molecules, chemical species (oxygen, ions, etc.) and the higher volume allows the formation of stable products between successive hydroxyl radical attack. Translating this process in AIMD is not simple and requires a compromise due to the computational power needed to take into account these parameters. As such, some of the degradation products (Table 1) are organic radicals and peroxides, which could represent the unstable intermediaries of chemical reaction, which cannot be experimentally detected. Thus, the main advantage of the AIMD method is the insight into the chemical reactions and its complementarity towards the experimental results.

6 | CONCLUSIONS

AIMD simulations are conducted for providing prediction of degradation products in water by HO• radical. It consists of releasing periodically HO• radical in a simulation box containing one organic pollutant molecule (here phenol or SMX) surrounded by enough water molecules for mimicking the pollutant molecule in aqueous environment. This method has been validated by reproducing the first step of phenol hydroxylation. The second step of hydroxylation provides additional products compared to literature knowledge. Applying the methodology, defined for phenol, to SMX antibiotic molecule, leads to hydroxylation steps with 1, 2 and 3 HO• radicals, well reproducing plasma ozonation experiments as well as experiments from literature. Going further to SMX fragmentation, the plasma experiments fail to correlate to the AIMD results. Nevertheless, expanding the comparison to include fragments reported in the literature, provides additional agreements between AIMD and experiments. The differences between experiments and simulations can originates from too short simulation times preventing relaxation of intermediates compounds. They can also stem from the fact that AIMD simulations only consider HO• radical interactions with pollutant molecules, and thus do not account for other reactive species simultaneously produced in the experiments. Thus, the methodology can be successfully applied in order to predict the initial attacks of hydroxyl radicals on the organic pollutant molecule, as well as gain insight into the mechanistic aspects of the reactions. These results are promising, considering that the first change to the chemical structure of a target compound is what most studies consider pollutant removal. This method can be employed for all advanced oxidation processes, which are based on hydroxyl radical reactions. The same procedure can be easily extended to other active species produced by cold atmospheric plasmas (O_3, O•, NO_x,etc) both neutral and ions.

ACKNOWLEDGMENTS

Part of this work has been supported by Conseil Régional Centre-Val de Loire with grant #2021-00144786 for project Perturb'Eau. The experimental work was supported by a grant of the Romanian Ministry of Education and Research, CNCS - UEFISCDI, project number PN-III-P4-ID-PCE-2020-0335, within PNCDI III.

Author contributions

Pascal Brault built and ran simulations, wrote simulation parts and draft of the manuscript. Florin Bilea conducted the experiments and write experimental parts of the manuscript. Monica Magureanu and Corina Bradu supervised the experiments and contributed to the writing of the manuscript. Olivier Aubry, Dunpin Hong and Hervé Rabat contributed to the writing of the manuscript.

Financial disclosure

None reported.

Conflict of interest

The authors declare no potential conflict of interests.

References

[1] Pascal Brault, Mado Abraham, Aïda Bensebaa, Olivier Aubry, Dunpin Hong, Hervé Rabat, Monica Magureanu, *Journal of Applied Physics* **2021**, *129* (18), 183304.

[2] Peter Bruggeman, Daan C Schram, *Plasma Sources Science and Technology* **2010**, *19* (4), 045025.

[3] Patrick Vanraes, Annemie Bogaerts, *Applied Physics Reviews* **2018**, *5* (3), 031103.

[4] M. Magureanu, F. Bilea, C. Bradu, D. Hong, *Journal of Hazardous Materials* **2021**, *417*, 125481.

[5] Nadia Morin-Crini, Eric Lichtfouse, Marc Fourmentin, Ana Rita Lado Ribeiro, Constantinos Noutsopoulos, Francesca Mapelli, Éva Fenyvesi, Melissa Gurgel Adeodato Vieira, Lorenzo A. Picos-Corrales, Juan Carlos Moreno-Piraján, Liliana Giraldo, Tamás Sohajda, Mohammad Mahmudul Huq, Jafar Soltan, Giangiacomo Torri, Monica Magureanu, Corina Bradu, Grégorio Crini, *Environmental Chemistry Letters 2022 20:2* **2022**, *20* (2), 1333–1375.

[6] Maria Klavarioti, Dionissios Mantzavinos, Despo Kassinos, *Environment International* **2009**, *35* (2), 402–417.

[7] Mehmet A Oturan, Jean-Jacques Aaron, *Critical Reviews in Environmental Science and Technology* **2014**, *44* (23), 2577–2641.

[8] E.C. Neyts, P. Brault, *Plasma Processes and Polymers* **2017**, *14* (1-2), 1600145.

[9] Michael Bonitz, Alexey Filinov, Jan Willem Abraham, Karsten Balzer, Hanno Kählert, Eckhard Pehlke, Franz X. Bronold, Matthias Pamperin, Markus Becker, Dettlef Loffhagen, Holger Fehske, *Frontiers of Chemical Science and Engineering 2019 13:2* **2019**, *13* (2), 201–237.

[10] Mohammad Zarshenas, Konstantin Moshkunov, Bartlomiej Czerwinski, Tom Leyssens, Arnaud Delcorte, *The Journal of Physical Chemistry C* **2018**, *122* (27), 15252–15263.

[11] Pascal Brault, Marisol Ji, Dario Sciacqua, Fabienne Poncin-Epaillard, Johannes Berndt, Eva Kovacevic, *Plasma Processes and Polymers* **2022**, *19* (1), 2100103.

[12] G Tetard, A Michau, S Prasanna, J Mougenot, P Brault, K Hassouni, *Plasma Sources Science and Technology* **2021**, *30* (10), 105015.

[13] Gautier Tetard, Armelle Michau, Swaminathan Prasanna, Jonathan Mougenot, Pascal Brault, Khaled Hassouni, *Plasma Processes and Polymers* **2022**, *19* (5), 2100204.

[14] Tao Liang, Yun Kyung Shin, Yu Ting Cheng, Dundar E. Yilmaz, Karthik Guda Vishnu, Osvalds Verners, Chenyu Zou, Simon R. Phillpot, Susan B. Sinnott, Adri C.T. Van Duin, *Annual Review of Materials Research* **2013**, *43*, 109–129.

[15] D Marx, J Hutter, *Ab Initio Molecular Dynamics: Theory and Implementation, in Modern Methods and Algorithms of Quantum Chemistry*, *Vol. 22*, Publication Series of the John von Neumann Institute for Computing J Grotendorst (Ed.), **2004**.

[16] Stefan Grimme, Christoph Bannwarth, Philip Shushkov, *Journal of Chemical Theory and Computation* **2017**, *13* (5), 1989–2009.

[17] Namita Panigrahy, Ankita Priyadarshini, Mitali Madhusmita Sahoo, Akshaya Kumar Verma, Achlesh Daverey, Naresh Kumar Sahoo, *Environmental Technology & Innovation* **2022**, *27*, 102423.

[18] Robert M Bruce, Joseph Santodonato, Michael W Neal, *Toxicology and Industrial Health* **1987**, *3* (4), 535–568.

[19] Wan Qian Guo, Ren Li Yin, Xian Jiao Zhou, Juan Shan Du, Hai Ou Cao, Shan Shan Yang, Nan Qi Ren, *Ultrasonics Sonochemistry* **2015**, *22*, 182–187.

[20] Kil Seong Kim, Sang Kyu Kam, Young Sun Mok, *Chemical Engineering Journal* **2015**, *271*, 31–42.

[21] G. Prasannamedha, P. Senthil Kumar, *Journal of Cleaner Production* **2020**, *250*, 119553.

[22] Lúcia H.M.L.M. Santos, Meritxell Gros, Sara Rodriguez-Mozaz, Cristina Delerue-Matos, Angelina Pena, Damià Barceló, M. Conceição B.S.M. Montenegro, *Science of The Total Environment* **2013**, *461-462*, 302–316.

[23] Manvendra Patel, Rahul Kumar, Kamal Kishor, Todd Mlsna, Charles U. Pittman, Dinesh Mohan, *Pharmaceuticals of emerging concern in aquatic systems: Chemistry, occurrence, effects, and removal methods*, **2019**.

[24] Phong K. Thai, Le Xuan Ky, Vu Ngan Binh, Pham Hong Nhung, Pham Thi Nhan, Ngo Quang Hieu, Nhung T.T. Dang, Nguyen Kieu Bang Tam, Nguyen Thi Kieu Anh, *Science of The Total Environment* **2018**, *645*, 393–400.

[25] Haiyang Chen, Lijun Jing, Yanguo Teng, Jinsheng Wang, *Science of The Total Environment* **2018**, *618*, 409–418.

[26] Marie Claire Danner, Anne Robertson, Volker Behrends, Julia Reiss, *Science of The Total Environment* **2019**, *664*, 793–804.

[27] Yaru Hu, Lei Jiang, Tianyang Zhang, Lei Jin, Qi Han, Dong Zhang, Kuangfei Lin, Changzheng Cui, *Journal of Hazardous Materials* **2018**, *360*, 364–372.

[28] T. Soini R. Rüger, M. Franchini, T. Trnka, A. Yakovlev, E. van Lenthe, P. Philipsen, T. van Vuren, B. Klumpers, *AMS2022.1*, **2022**. http://www.scm.com/.

[29] D. Dobrin, M. Magureanu, C. Bradu, N. B. Mandache, P. Ionita, V. I. Parvulescu, *Environmental Science and Pollution Research* **2014**, *21*, 12190–12197.

[30] C. Bradu, M. Magureanu, V. I. Parvulescu, *Journal of Hazardous Materials* **2017**, *336*, 52–56.

[31] M Magureanu, D Dobrin, C Bradu, F Gherendi, N B Mandache, V I Parvulescu, *Chemosphere* **2016**, *165*, 507–514.

[32] F Bilea, C Bradu, N B Mandache, M Magureanu, *Chemosphere* **2019**, *236*, 124302.

[33] Monica Magureanu, Nicolae Bogdan Mandache, Corina Bradu, Vasile I. Parvulescu, *Plasma Processes and Polymers* **2018**, *15* (6), 1700201.

[34] Jorge Villaseñor, Patricio Reyes, Gina Pecchi, *Catalysis Today* **2002**, *76* (2-4), 121–131.

[35] Bruce R. Locke, Petr Lukes, Jean Louis Brisset, *Plasma Chemistry and Catalysis in Gases and Liquids* **2012**, 185–241.

[36] M. N. Abellán, B. Bayarri, J. Giménez, J. Costa, *Applied Catalysis B: Environmental* **2007**, *74* (3-4), 233–241.

[37] Jan O. Back, Thomas Obholzer, Karl Winkler, Simon Jabornig, Marco Rupprich, *Journal of Environmental Chemical Engineering* **2018**, *6* (6), 7377–7385.

[38] Donggwan Lee, Jae Cheol Lee, Joo Youn Nam, Hyun Woo Kim, *Chemosphere* **2018**, *209*, 901–907.

[39] Emile Salomon Massima Mouele, Tay Zar Myint Myo, Htet Htet Kyaw, Jimoh O Tijani, Mihaela Dinu, Anca C Parau, Iulian Pana, Youssef El Ouardi, Jamal Al-Sabahi, Mohammed Al-Belushi, Eduard Sosnin, Victor Tarasenko, Cheng Zhang, Tao Shao, Tanta Verona Iordache, Sandu Teodor, Katri Laatikainen, Alina Vladescu, Mohammed Al-Abri, Andrei Sarbu, Mariana Braic, Viorel Braic, Sergey Dobretsov, Leslie F Petrik, *Journal of Hazardous Materials Advances* **2022**, *5*, 100051.

[40] Kefeng Shang, Rino Morent, Ning Wang, Yongxin Wang, Bangfa Peng, Nan Jiang, Na Lu, Jie Li, *Chemical Engineering Journal* **2022**, *431*, 133916.

[41] Yawen Wang, Jingwen Huang, He Guo, Chendong Puyang, Jiangang Han, Yan Li, Yunxia Ruan, *Separation and Purification Technology* **2022**, *287*, 120540.

[42] Kien Tiek Wong, So Yeon Yoon, Seok Byum Jang, Nurhaslina Abd Rahman, Choe Earn Choong, Young June Hong, Sang Eun Oh, Eun Ha Choi, Min Jang, *Chemosphere* **2023**, *311*, 137003.

[43] Huihui Zhang, Sisi Xiao, Yansheng Du, Shilin Song, Kun Hu, Yuyue Huang, Huijuan Wang, Qiangshun Wu, *Separation and Purification Technology* **2022**, *298*, 121608.

[44] Ai Zhang, Yongquan Zhou, Yongmei Li, Yanbiao Liu, Xiang Li, Gang Xue, Andere Clement Miruka, Ming Zheng, Yanan Liu, *Water Research* **2022**, *212*, 118128.

[45] Florin Bilea, Tian Tian, Monica Magureanu, Hervé Rabat, Mohamed-Ali Antoissi, Olivier Aubry, Dunpin Hong, *Plasma Processes and Polymers*, *n/a* (n/a), e2300020.

[46] Jéssica Martini, Carla A. Orge, Joaquim L. Faria, M. Fernando R. Pereira, O. Salomé G.P. Soares, *Journal of Environmental Chemical Engineering* **2018**, *6* (4), 4054–4060.

[47] P J Bruggeman, M J Kushner, B R Locke, J G E Gardeniers, W G Graham, D B Graves, R C H M Hofman-Caris, D Maric, J P Reid, E Ceriani, D Fernandez Rivas, J E Foster, S C Garrick, Y Gorbanev, S Hamaguchi, F Iza, H Jablonowski, E Klimova, J Kolb, F Krcma, P Lukes, Z Machala, I Marinov, D Mariotti, S Mededovic Thagard, D Minakata, E C Neyts, J Pawlat, Z Lj Petrovic, R Pflieger, S Reuter, D C Schram, S Schröter, M Shiraiwa, B Tarabová, P A Tsai, J R R Verlet, T von Woedtke, K R Wilson, K Yasui, G Zvereva, *Plasma Sources Science and Technology* **2016**, *25* (5), 053002.